JOURNAL OF THE MECHANICAL BEHAVIOR OF BIOMEDICAL MATERIALS 57 (2016) 149–156

Available online at www.sciencedirect.com

ScienceDirect

www.elsevier.com/locate/jmbbm


Research paper

# Fatigue behavior of Y-TZP ceramic after surface treatments

*Marina Amaral*[a], *Paulo Francisco Cesar*[b], *Marco Antonio Bottino*[a], *Ulrich Lohbauer*[c], *Luiz Felipe Valandro*[d,*]

[a]*Department of Dental Materials and Prosthesis, Dentistry School, Sao Paulo State University, Av. Eng Franscisco José Longo, 777, Sao Jose dos Campos, Brazil*

[b]*Department of Dental Materials, Dentistry School, Sao Paulo University, Av. Prof Lineu Prestes, 2227 Sao Paulo, Brazil*

[c]*Head of the Laboratory for Biomaterials Research, Dental Clinic 1 – Operative Dentistry and Periodontology, University of Erlangen-Nuernberg, Glueckstrasse, 11, Erlangen, Germany*

[d]*Department of Restorative Dentistry, Dentistry School, Prosthodontic Unit, Federal University of Santa Maria, Rua Marechal Floriano Peixoto, 1184, 97015-372 Santa Maria, Rio Grande do Sul, Brazil*

ARTICLE INFO

*Article history:*
Received 2 September 2015
Received in revised form
20 November 2015
Accepted 25 November 2015
Available online 15 December 2015

*Keywords:*
Zirconia ceramic
Fatigue
Surface treatments
Strength
Weibul analysis

ABSTRACT

*Objectives:* The aim of this study was to evaluate the effect of three surface treatments on the biaxial flexural strength before and after mechanical cycling, and fatigue limit of a Y-TZP ceramic.

*Methods:* Disc-shaped specimens were produced and three surface conditions were tested: CT (as-sintered, untreated), GL (thin layer of porcelain glaze), and AA (air abrasion with 30 μm silica particles). Profilometric and phase transformation analyses were performed. Disks were submitted to biaxial flexural strength (BFS) before and after mechanical cycling (100 N, $2 \times 10^6$ cycles) and staircase approach ($n=20$). The flexural fatigue limits (FFLs) were obtained at $10^2$, $10^3$, $10^4$ and $10^5$ cycles.

*Results:* Tetragonal to monoclinic transformation was only observed for AA group (9.46% of monoclinic phase). Glazed group presented the highest Ra values. Flexural strength was higher for AA group; CT and GL groups were similar. The reliability was similar between groups. The mechanical cycling at 100 N did not affected flexural strength. FFLs were higher for AA group, and the three surface treatments presented decrease in strength according to the increase in number o cycles.

© 2015 Elsevier Ltd. All rights reserved.

## 1. Introduction

Y-TZP ceramic (Yttria-stabilized tetragonal zirconia polycrystal) has a large number of indications in restorative and implant dentistry, like frameworks or monolithic restorations for fixed dental prostheses (FDP) and single crowns, implant abutments, inlay- and onlay-bridges. The great popularity of this ceramic material is related to the advantages in its

*Corresponding author. Tel.: +55 55 3220 9276; fax: +55 55 3220 9272.
E-mail addresses: marinamaral_85@yahoo.com.br (M. Amaral), paulofc@usp.br (P.F. Cesar), mmbottino@uol.com.br (M.A. Bottino), ulrich.lohbauer@fau.de (U. Lohbauer), lfvalandro@hotmail.com (L.F. Valandro).

http://dx.doi.org/10.1016/j.jmbbm.2015.11.042
1751-6161/© 2015 Elsevier Ltd. All rights reserved.

esthetic characteristics and the superior mechanical properties compared to metal and other dental ceramics (Ban et al., 2007; Guazzato et al., 2004). Although ceramics are susceptible to brittle fracture, which is particularly difficult to predict. Clinical evaluations showed high success rates of all-ceramic restorations with zirconia-based infra-structures (Näpänkangas et al., 2015). Nevertheless there is still some concern regarding the reliability of monolithic Y-TZP systems, as the follow-up periods reported are relatively short, varying from 6 to 18 months (Batson et al., 2014; Chang et al., 2015; Stober et al., 2014).

Establishing good adhesion between resin cements and Y-TZP restorations is clinically imperative in clinical situations, like inlay retained bridges, and less retentive dental abutments. With the introduction of phosphate monomers (MDP) into bonding primers and adhesives, a durable chemical bonding to zirconia could be achieved (Amaral et al., 2014). However, mechanical retention still improves the bonding performance of resin cements to Y-TZP ceramic (Aboushelib et al., 2010; Kitayama et al., 2009; Vanderlei et al., 2014).

Previous investigations demonstrated that the association of silica deposition and silane application on the surface of Y-TZP results in high and long-lasting bond strength between Y-TZP and resin cement (Aboushelib et al., 2010, 2008, 2011). However, surface treatments may be deleterious for the long term mechanical behavior of the restorations, as they may introduce multiple surface damages (Guess et al., 2010; Cattell et al., 2009; Luthardt et al., 2004; Wang et al., 2008). The work from Scherrer et al. (2011) is one of the few studies showing a beneficial effect of air abrasion (30 μm silica particles, 2.5 bar, 20 s) on the mechanical fatigue behavior of Y-TZP after ageing in humid environment.

The application of a thin low-fusing glassy layer (rich in silicon oxides) on the cementation surface of the ceramic, followed by hydrofluoric acid etching and silane application has been investigated as an alternative surface treatment and showed promising results with significant improvements of the bond strength between resin cements and Y-TZP (Aboushelib et al., 2010; Kitayama et al., 2009; Vanderlei et al., 2014; Ntala et al., 2010). On the other hand, some studies indicated that, under tensile stresses, this glassy layer might undergo crack initiation and propagation with subsequent decrease in structural reliability of the specimens (Guazzato et al., 2004; Hjerppe et al., 2010).

Defects may lead to sites of stress concentration, which may overcome the effects of the compressive layer created by the tetragonal to monoclinic phase transformation, and favor fracture. Furthermore, glass-based materials are more brittle and susceptible to slow crack growth in humid environment than zirconia (Borba et al., 2011; Taskonak et al., 2008). The presence of stresses at the crack tip and the corrosion caused by water reduces the surface energy at the crack tip and causes crack propagation. These cracks grow continuously under loads lower than the critical, until leading to catastrophic failure of the ceramic restoration (slow crack growth). The effects of surface treatments on the SCG of zirconia restorations, and the reliability of the material still need to be determined (Guess et al., 2010; Luthardt et al., 2004; Wang et al., 2008; Scherrer et al, 2011; Kosmac et al., 2008).

Since clinically failed Y-TZP crowns had the failure origin located on the cementation surface, where the greatest tensile stresses were concentrated (Aboushelib et al., 2008), the aim of this study was to evaluate the influence of three surface treatments on the initial strength, fatigue limit and failure mode of one Y-TZP ceramic. The null hypothesis tested was that the surface treatments would not affect the strength and fatigue behavior of the Y-TZP.

## 2. Material and methods

### 2.1. Specimen preparation

Pre-sintered blocks of Y-TZP ceramic (VITA In-Ceram YZ, VITA Zahnfabrik, Bad Säckingen, Germany) were hand-ground into cylinders (15 mm in diameterx40 mm in length) and sectioned into 1.8 mm-thick slices. Disks were polished in both surfaces with 1200 grit sandpaper, cleaned in ultrasonic bath with alcohol for 5 min, and sintered (1530 °C, holding time of 120 min) in a specific furnace (VITA Zyrcomat T, VITA Zahnfabrik). The final dimensions of the disc-shaped specimens were 12 mm in diameter and 1.2 mm in thickness (ISO 6872-2008).

Three surface treatments were then performed: (1) specimens were kept as-sintered, without any surface modification after firing (CT), (2) specimens were air-abraded with 30 μm silica-modified particles (Rocatec Soft, 3M ESPE, USA) at 2.5 bar pressure, during 20 s, at 10 mm distance (AA), and (3) a thin layer of glassy glaze (AKZENT VITA Glaze, VITA Zahnfabrik) was applied to the Y-TZP surface, fired (900 °C/1 min) and etched with hydrofluoric acid (5%/1 min) (GL).

### 2.2. Profilometric analysis

Three specimens ($n=3$) from each group were observed on a high-resolution non-contact confocal white-light profilometer (CyberSCAN CT 100, Cyber Technologies GmbH, Ingolstadt, Germany), to determine the surface pattern and mean roughness (Ra values). For each specimen an area of 1 $mm^2$ was scanned with a 0.02 μm resolution sensor head in 10 $\mu m^2$ step-sizes for 2 ms illumination time each. In this technique, the height levels are detected over a measurement range defined by different wavelengths within the projected white light beam spectrum. Changes in the intensity and wavelength are analyzed by the spectrometer, which defines height levels as they reach the maximum intensity level for a specific wavelength. Reflection intensities were selected to prevent interference from sub-surface signals for a clean reading of light reflections coming uniquely from the surface of translucent materials.

### 2.3. Crystalline phase analysis

Specimens ($n=2$) were analyzed under an X-ray diffractometer (PW 1830, Philips, Amsterdam, The Netherlands) to determine the amount of m-phase under each condition of surface treatment. Spectra were collected in the $2\theta$ range 25–35°, step interval of 1 s; step size of 0.03°. The amount of m-phase was calculated according to Toraya et al. (1984).

### 2.4. Mechanical tests

The initial flexural strength was calculated through a biaxial flexural test. Disks ($n=20$) were positioned with the treated surface on the tensile side over three support balls (Ø=3.2 mm) positioned 10 mm apart from each other in a triangular position. The assembly was immersed in water, and a flat circular tungsten piston (Ø=1.6 mm) was used to apply an increasing load (1 mm/min) until catastrophic failure. Before the test, an adhesive tape ($12\times10$ mm$^2$, 3M ESPE) was fixed on the compression side of the disks to avoid spreading of the fragments (Quinn, 2007) and to provide better contact between the piston and the specimen. Flexural strength was calculated according to ISO 6872-2008. The flexural strength was measured in the same way, after mechanical cycling ($n=20$). Disks were first subjected to $2\times10^6$ cycles (4 Hz) of 100 N load (ERIOS 11000 Fatigue Machine, ERIOS, Sao Paulo, Brazil), immersed in water at 37 °C, in a biaxial flexural test configuration, simulating about 2 years of clinical use (Wiskott et al., 1995).

The flexural fatigue limits were determined through staircase approach for $10^2$, $10^3$, $10^4$ and $10^5$ cycles at a frequency of 0.5 Hz ($n=20$) (Z 2.5, Zwick, Ulm, Germany). The first specimen was tested at approximately 70% of the respective initial flexural strength values (initial load in monotonic tests). For every cycle the stress alternated from 3 MPa to the maximum stress. The test was conducted sequentially, with the maximum applied stress being increased or decreased by a fixed load increment (5% of the initial load) according to whether the previous test resulted in failure or not.

### 2.5. Failure analysis

Fractographic examination was performed under a light microscope on representative specimens (total of 36 samples – 2 per group; samples from initial strength with and without mechanical cycling, and from staircase test). The aim of this analysis was to identify the fracture origin and classify it according to the location into three types (Quinn, 2007): (1) volume located (higher resistance to crack propagation), (2) surface located (lower resistance to crack propagation) or (3) near-surface located (higher resistance to crack propagation than type 2). Scanning electron microscopy was conducted on representative specimens.

### 2.6. Data analysis

A two-way analysis of variance was performed to compare flexural strength data from load-to-fracture test. The Weibull parameter $m$ (modulus) and $\sigma_0$ (characteristic strength) were determined by plotting the following diagram (according to ENV 843-5):

$$\ln\ln 1/1-F_{(\sigma c)} = m\ln\sigma_c - m\ln\sigma_0 \quad (1)$$

The characteristic strength ($\sigma_0$) is considered to be the strength at a failure probability of approximately 63%, and the Weibull modulus ($m$) is used as a measure of the distribution of the strength values, which expresses the reliability of the material. The scale parameter ($\sigma_0$) was estimated also for failure probability of 5%, which is considered to be more clinically relevant in dentistry (Teixeira et al., 2007).

The fatigue limits (FFLs) for $10^2$, $10^3$, $10^4$ and $10^5$ cycles and respective standard deviations (SD) were calculated according to Eqs. (2) and (3).

$$\mathrm{FFL} = X_0 + d\left[\left(\sum in_i/\sum n_i\right)\pm 0.5\right] \quad (2)$$

$$\mathrm{SD} = 1.62d\left\{\left[\left(\sum n_i\sum i^2n_i - \left(\sum in_i\right)^2/\left(\sum n_i\right)^2\right)\right] + 0.029\right\} \quad (3)$$

where $X_0$ is the lowest stress level considered in the analysis and $d$ is the fixed stress increment. In Eq. (2) the negative sign is used when the less frequent event is failure, otherwise the positive sign is used. $i=0$ represents the lowest stress level considered, followed by $i=1$, and so on; and $n_i$ is the number of failures or non-failures at the given stress level. The confidence intervals (CI) (95%) were calculated according to Collin's method (Collins, 1993) and the statistical difference is given by the non-overlapping of the CI.

## 3. Results

The profilometric analysis showed mean roughness value (Ra) of 0.29 μm (±0.03) for the control group, 0.31 μm (±0.04) for the air-abraded group, and 0.63 μm (±0.1) for the glazed group. Specimens from control and glazed groups did not show tetragonal-to-monoclinic phase transformation. However, after air-abrasion (AA group), the monoclinic phase content measured on the Y-TZP surface was 9.5%.

The single load-to-failure mean values (FS) are displayed in Table 1, along with the Weibull parameters (characteristic strength, $\sigma_0$, and Weibull modulus, $m$). Mechanical cycling did not influence FS values ($p=0.133$), but surface treatment did ($p<0.001$). The FS and $\sigma_0$ values of the control and glazed groups were statistically similar and significantly lower than that obtained for the air-abraded group. There was no statistical difference among the Weibull moduli obtained for the three experimental groups when specimens that were not subjected to mechanical cycling were compared. The $m$-value of the group GL/MC was similar to that of GL, and higher than those of the other tested groups. Mechanical cycling at 100 N-load did not cause significant change in the FS, characteristic strength and Weibull modulus of any of the experimental groups.

Fatigue limits (FFLs) obtained for each surface treatment as a function of the number of cycles are displayed in Table 2. Values were higher for the air-abraded group in comparison to the other groups (no overlapping of CI) regardless of the number of cycles. The AA group submitted to $10^2$ cycles showed higher value of FFL compared to AA specimens after $10^3$, $10^4$ and $10^5$ cycles. The same was observed in glazed group: GL($10^2$) > GL($10^3$) = GL($10^4$) = GL($10^5$). Fig. 1 represents the values plotted in a graph, with a best-fit curve between FFLs. The degradation rates were similar for the glazed and air-abraded groups (note similar slope in Fig. 1); the control group showed the lowest downward slope of the curve after 100 cycles.

**Table 1 – Results of flexural strength and respective standard deviation (MPa) (FS ± SD), characteristic strength ($\sigma_0$), Weibull modulus ($m$), respective confidence intervals (CI), and strength values to 5% of failure probability ($\sigma_{5\%}$).**

| Group[a] | FS ± SD | $\sigma_0$ | C.I. | $m$ | C.I. | $\sigma_{5\%}$ |
|---|---|---|---|---|---|---|
| CT | $922.3^{B} \pm 97.40$ | $965.1^{B}$ | 918.5–1013.3 | $11.1^{C}$ | 7.0–14.9 | 738.3 |
| CT/MC | $1012^{B} \pm 134.7$ | $1071.0^{B}$ | 1003.8–1141.9 | $9.01^{C}$ | 5.5–12.3 | 770.3 |
| AA | $1258^{A} \pm 191.2$ | $1343.5^{A}$ | 1239.7–1454.7 | $7.30^{C}$ | 4.5–9.9 | 892.7 |
| AA/MC | $1248^{A} \pm 167.3$ | $1319.1^{A}$ | 1234.1–1409.1 | $8.80^{C}$ | 5.4–11.9 | 939.9 |
| GL | $997.3^{B} \pm 90.80$ | $1040.3^{B}$ | 991.3–1091.1 | $12.1^{BC}$ | 7.4–16.5 | 896.1 |
| GL/MC | $1044^{B} \pm 48.40$ | $1065.5^{B}$ | 1042.1–1089.3 | $26.2^{AB}$ | 16.1–35.7 | 951.4 |

Different uppercase letters indicate statistical difference into the columns.
[a] MC = Mechanical cycling: $2x10^6$ cycles of 100 N load.

**Table 2 – Mean initial strength, FFLs, confidence intervals according to Collin's method and percentage of decrease in strength.**

| Groups | Initial mean strength (MPa) | Number of cycles | FFL (SD) (MPa) | CI (95%) Collin's Method | % of FFL decrease |
|---|---|---|---|---|---|
| CT | 922.3 | $10^2$ | 817.00 (59.01) | 781.83–852.17 | 11.4 |
| | | $10^3$ | 784.77 (52.69) | 755.38–813.48 | 14.9 |
| | | $10^4$ | 769.47 (79.07) | 727.06–808.27 | 16.6 |
| | | $10^5$ | 777.00 (26.61) | 758.00–796.00 | 15.8 |
| AA | 1258 | $10^2$ | 1147.1 (19.52) | 1128.3–1165.9 | 8.84 |
| | | $10^3$ | 1096.9 (39.89) | 1067.3–1126.4 | 12.8 |
| | | $10^4$ | 1072.5 (27.68) | 1050.9–1094.1 | 14.8 |
| | | $10^5$ | 1023.0 (122.3) | 949.24–1096.8 | 18.7 |
| GL | 997.3 | $10^2$ | 912.50 (47.93) | 879.48–945.52 | 8.50 |
| | | $10^3$ | 835.63 (29.11) | 814.85–856.40 | 16.2 |
| | | $10^4$ | 826.88 (64.55) | 788.41–865.34 | 17.1 |
| | | $10^5$ | 799.17 (14.24) | 739.78–773.97 | 19.9 |

The number of disc fragments obtained after the fracture event were computed and correlated with the maximum applied stresses. Pearson's correlation test showed that there was significant correlation between these variables. The correlation was considered as moderate in both cases: initial flexural strength, before or after MC ($r^2=0.896$) and flexural fatigue limit test ($r^2=0.701$).

Fig. 2 shows representative micrographs of fractured surfaces. Samples from the air-abraded group had most part of the failures located right below the tensile surface – type 3 (Fig. 2B), while for the control (Fig. 2A) and glazed groups (Fig. 2C) the origin was more frequently located right at the tensile surface (type 2) of the flexural disc. Fractography did not reveal signs of crack growth in any of the fracture surfaces after $10^4$ cycles (Fig. 3).

## 4. Discussion

This study evaluated the flexural strength before and after mechanical cycling, and the fatigue limits of surface-treated Y-TZP disks. The hypothesis that surface treatments would not affect the flexural strength and fatigue behavior of Y-TZP disks was rejected, since the results showed that both the Weibull parameters and FFLs of the Y-TZP varied significantly depending on the surface condition.

The higher flexural strength results obtained for the air-abraded group are probably related to the tetragonal-to-monoclinic phase transformation that takes place after air abrasion (9.5 vol% of monoclinic phase), and the absence of this transformation in both the control and glazed groups (0.0%). The phase transformation phenomenon creates a superficial compression layer, as a consequence of the 4–5% volume increase of the zirconia crystal, leading to a tougher surface layer and consequently higher initial flexural strength values (Zhang et al., 2004; Borchers et al., 2010).

Samples were submitted to air-abrasion with silica-modified particles of 30 μm, which is a relatively small particle size. The fact that control and AA groups presented roughness values near to each other could be used to partially explain why particle abrasion did not decrease the flexural strength. It seems that the surface was not extensively damaged by sandblasting. Probably the defects were not sufficiently deep enough to overcome the compressive layer (Zhang et al., 2006) – about 0.5 μm-thick (Souza et al., 2013; Amaral et al., 2013). This value was calculated according to Kosmac et al. (1981) and was based on the amount of monoclinic phase, and took into account that a constant fraction of grains had symmetrically transformed along the surface. The decrease in the FFL values was only significant between $10^2$ and $10^3$ cycles. After $10^3$, $10^4$ and $10^5$ cycles, the FFL values were similar.

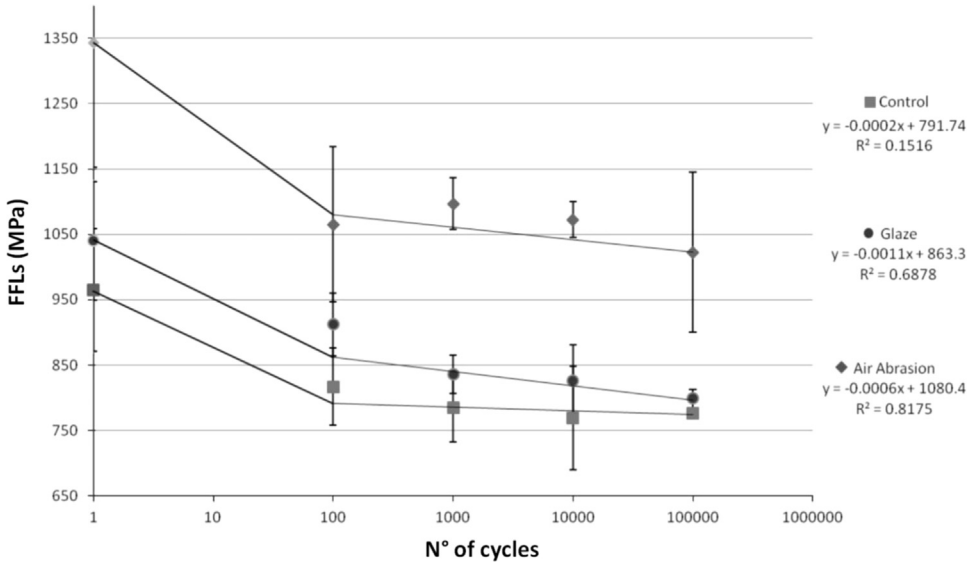


**Fig. 1 – Best-fitting curves for FFLs values and initial strength (at 1 cycle) from each group, representing the degradation pattern of the ceramic in each situation.**

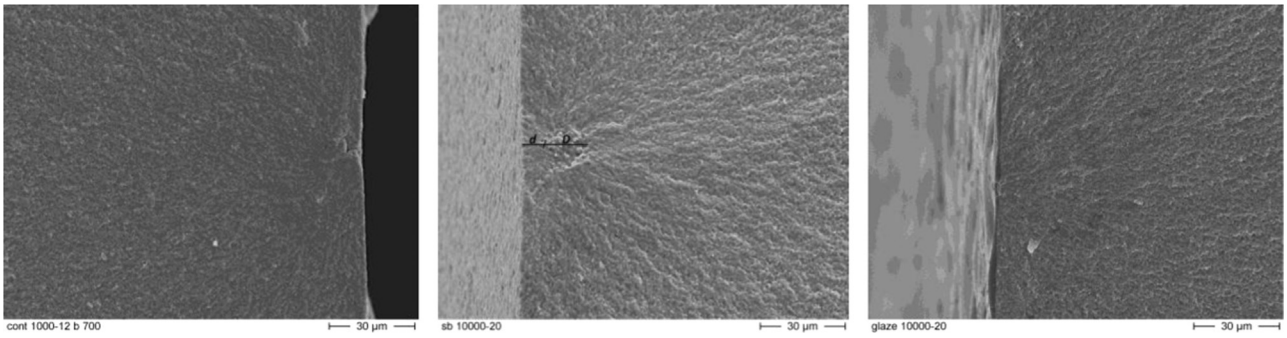


**Fig. 2 – Representative images of fracture surfaces from control, air abraded and glazed groups, from left to right, respectively. Control and glazed groups presented the failure origin located at the surface, and air abraded presented the failure located near the surface (distance from origin to surface) (*d*) < diameter of the defect (D). No volume-located failure was observed.**

Characteristic strength and Weibull modulus were not affected by mechanical cycling with the load of 100 N. The high *m* value obtained for the glazed group after mechanical cycling (Table 1) may be attributed to a protective glassy layer created at the zirconia surface, which protected the material from water corrosion during the test (2 weeks immersed in water). The load of 100 N (corresponding in this case to approximately 200 MPa) was not enough to affect the mechanical behavior of Y-TZP, even after a relatively high-number of cycles (2,000,000). The 100 N-load used during mechanical cycling is in the range of normal chewing loads. However, the tensile stresses generated in the specimens of the current investigation were relatively low, as they are only 8–12% of the initial biaxial strength of the groups (Table 2). It is likely that such stress level is below critical threshold for slow crack propagation of defects in this material.

When the number of cycles increased in staircase approach (from 100 to 100,000), the FFL values decreased. In Fig. 1, it is clear that, for all tested groups, the greater drop in the fatigue limit was between 1 and 100 cycles (decrease of ~8.5% to 11.4%). After that point, the decrease was significant for GL and AA group. This fact indicates that the higher decrease in strength takes place after a small number of cycles (Mitov et al., 2011; Scherrer et al., 2011; Borba et al., 2011), when the material is subjected to relatively high-stresses in the fatigue experiment. Below $10^5$ cycles, the applied load is high, and larger deformation of the material occurs at each cycle, resulting in a lower number of cycles performed before failure of the sample (low-cycle fatigue behavior) (Collins, 1993).

It is important to note that the previously mentioned phase transformation observed for the air-abraded group is also responsible for the high FFL values (Scherrer et al., 2011; Draughn, 1979). The AA group showed higher values of fatigue limit, than the other two surface treatments, regardless of the number of cycles applied (Table 2). Despite this good performance in terms of FFL, it should be highlighted that the decrease in the FFL values was significant between $10^2$ cycles and the other series of cycles only for surface-treated groups. Nevertheless, the decrease observed was relatively small when compared to other ceramic materials from the literature, as silica-based ceramics or resin composite (Belli et al., 2014). This fact is expressed by the higher

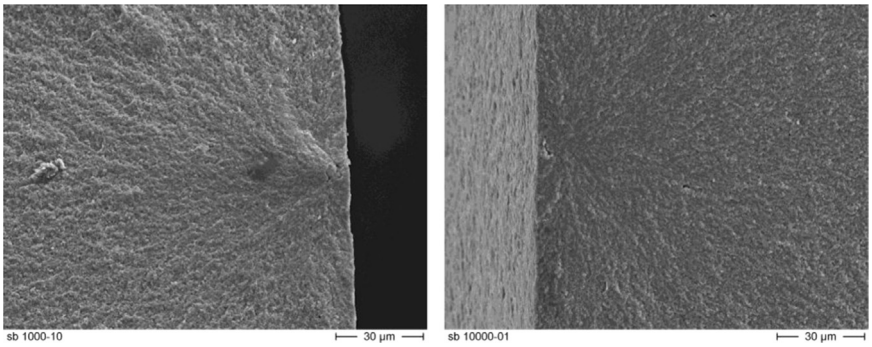


**Fig. 3 – Images from air abraded samples that failed after different number of cycles. (A) 4 cycles, applied stress: 1096.86 MPa; (B) 9.456 cycles, applied stress: 884.38 MPa.**

slope of the curves fitted on the data obtained for surface treated groups than for the control group (Fig. 1).

Fatigue failure of polycrystalline ceramics is controlled by slow crack growth (SCG) of pre-existing flaws (Ritter and Humenik, 1979). The prediction of strength degradation, represented by the best-fit curve in Fig. 1, showed a relatively stable slope after 100 cycles for the control group, indicating that this type of surface without sandblasting damages is not significantly influenced by the SCG phenomenon.

Under static conditions, subcritical crack growth is caused by stress corrosion at the crack tip caused by the dissociated $H_2O$ ions. Under mechanical cycling, the effects of the degradation of the transformation zone should also be considered, and therefore shorter lifetimes are expected, as compared to static conditions (Ritter and Humenik, 1979). The fatigue test in the present study was performed in humid environment and the test duration depended on the number of cycles, varying from 15 min (100 cycles) to 7 days ($10^5$ cycles). Hence, the longer exposition to humid environment might have contributed to the decrease in strength with the increase in number of cycles, as observed for surface-treated specimens. More specifically, the contact with water may be responsible for the steeper slope also observed for the glazed group, since it is well known (Morena et al., 1986) that water significantly decreases the strength of most glasses, acting chemically at crack tips and allowing the slow and stable growth of cracks before catastrophic failure (Quinn, 2007).

During processing and after surface treatments, lots of defects are created on the material surface. Under clinical circumstances, different types of damages and flaws may be created as a result of CAD/CAM milling procedures (Amaral et al., 2014; Luthardt et al., 2002) and may result in different clinical outcomes. The location of the failure origin in zirconia infrastructures is still under discussion in literature. Guess et al. (2010) presented clinically failed Y-TZP crowns with the failure origin located at the internal/cementation surface, in the occlusal region of the restoration, where the greatest tensile stress concentrates during chewing (Aboushelib et al., 2008), but other locations for the failure to start may happen.

In the present investigation, failure analysis showed that all samples fractured from the center to the periphery of the disc, with the main crack running between the support balls (Quinn, 2007), and the crack origin located on the tensile side. Pearson's correlation coefficient was considered moderate for the number of disc fragments and the stress to failure, considering specimens tested in both biaxial flexural strength and fatigue limit tests,. In other words, the higher the specimen strength, the higher the number of fragments generated after fracture. Failure origins were located at the surface in both the control and glazed groups. In the first case (Fig. 2A), the origins were probably processing flaws originated during cutting and grinding (Scherrer et al., 2011). Volume flaws that were exposed during processing were also seen, as shown in Fig. 2A (Quinn, 2007). Fracture origins located at the surface in the glazed group were most likely related to areas where the glaze layer was removed by acid etching (Fig. 2C). The removal of the glaze created defects that may have favored stress concentration at that site. The glaze layer had about 4.4 µm in thickness. The additional thickness of the glaze layer may explain the slightly higher strength in comparison to that of the control group.

After air abrasion, most of the failure origins were located near the surface and the distance between the critical flaw and the surface was not larger than the flaw diameter or major axis length (Fig. 2) (Quinn, 2007), probably due to the compression layer formed on the Y-TZP surface, as previously discussed. In this situation, the shape factor for the critical flaw is larger than that observed for surface flaws, and therefore the material will have increased capability to resist crack propagation. No signs of slow crack growth were recognized on the fracture surfaces, even for groups that received surface treatment and showed higher decrease in FFLs after a high number of cycles (Fig. 3).

## 5. Conclusion

The present study demonstrated that no decrease in strength or fatigue limits of Y-TZP was observed after surface treatments. Indeed, air-abrasion (30 µm silica-modified particles) resulted in higher flexural strength and increased the fatigue strength, while the reliability was similar to the other groups. The application of a thin glass layer did not increase the flexural strength of Y-TZP but slightly modified its fatigue behavior. For all tested groups, the fatigue limits decreased when the number of cycles was increased.

## Acknowledgments

Authors thanks FAPESP (process #2010/20077-0) and CAPES (process #8746-11-7) by financial support.

## REFERENCES

Aboushelib, M.N., Matinlinna, J.P., Salameh, Z., Ounsi, H., 2008. Innovations in bonding to zirconia-based materials: Part I. Dent. Mater. 24 (9), 1268–1272, http://dx.doi.org/10.1016/j.dental.2008.02.010.

Aboushelib, M.N., Feilzer, A.J., Kleverlaan, C.J., 2010. Bonding to zirconia using a new surface treatment. J. Prosthodont. 19 (5), 340–346, http://dx.doi.org/10.1111/j.1532-849X.2010.00575.x.

Aboushelib, M.N., 2011. Evaluation of zirconia/resin bond strength and interface quality using a new technique. J. Adhes. Dent. 13 (3), 255–260, http://dx.doi.org/10.3290/j.jad.a19241.

Amaral, M., Valandro, L.F., Bottino, M.A., Souza, R.O., 2013. Low-temperature degradation of a Y-TZP ceramic after surface treatments. J. Biomed. Mater. Res. B Appl. Biomater. 101 (8), 387–392, http://dx.doi.org/10.1002/jbm.b.32957.

Amaral, M., Belli, R., Cesar, P.F., Valandro, L.F., Petschelt, A., Lohbauer, U., 2014. The potential of novel primers and universal adhesives to bond to zirconia. J. Dent. 42 (1), 90–98, http://dx.doi.org/10.1016/j.jdent.2013.11.004.

Ban, S., Sato, H., Suehiro, Y., Nakanishi, H., Nawa, M., 2007. Effect of sandblasting and heat treatment on biaxial flexure strength of the zirconia/alumina nanocomposite. Key Eng. Mater. 330–332, 353–356, http://dx.doi.org/10.4028/www.scientific.net/KEM.330-332.353.

Batson, E.R., Cooper, L.F., Duqum, I., Mendonça, G., 2014. Clinical outcomes of three different crown systems with CAD/CAM technology. J. Prosthet. Dent. 112 (4), 770–777, http://dx.doi.org/10.1016/j.prosdent.2014.05.002.

Belli, R., Geinzer, E., Muschweck, A., Petschelt, A., Lohbauer, U., 2014. Mechanical fatigue degradation of ceramics versus resin composites for dental restorations. Dent. Mater. 30 (4), 424–432, http://dx.doi.org/10.1016/j.dental.2014.01.003.

Borba, M., de Araújo, M.D., Fukushima, K.A., Yoshimura, H.N., Cesar, P.F., Griggs, J.A., Bona, A. Della, 2011. Effect of the microstructure on the lifetime of dental ceramics. Dent. Mater. 27 (7), 710–721, http://dx.doi.org/10.1016/j.dental.2011.04.003.

Borchers, L., Stiesch, M., Bach, F.W., Buhl, J.C., Hübsch, C., Kellner, T., Kohorst, P., Jendras, M., 2010. Influence of hydrothermal and mechanical conditions on the strength of zirconia. Acta Biomater. 6 (12), 4547–4552, http://dx.doi.org/10.1016/j.actbio.2010.07.025.

Cattell, M.J., Chadwick, T.C., Knowles, J.C., Clarke, R.L., 2009. The development and testing of glaze materials for application to the fit surface of dental ceramic restorations. Dent. Mater. 25 (4), 431–441, http://dx.doi.org/10.1016/j.dental.2008.09.004.

Chang, J.S., Ji, W., Choi, C.H., Kim, S., 2015. Catastrophic failure of a monolithic zirconia prosthesis. J. Prosthet. Dent. 113 (2), 86–90, http://dx.doi.org/10.1016/j.prosdent.2014.07.016.

Collins, J.A., 1993. Fatigue testing procedures and statistical interpretations of data. In: Failure of Materials in Mechanical Design: Analysis, Prediction, Prevention. Second edition. Wiley-interscience. New York, pp. 374–392.

Draughn, R.A., 1979. Compressive fatigue limits of composite restorative materials. J. Dent. Res. 58 (3), 1093–1096, http://dx.doi.org/10.1177/00220345790580031101.

Guazzato, M., Albakry, M., Ringer, S.P., Swain, M.V., 2004. Strength, fracture toughness and microstructure of a selection of all-ceramic materials. Part II. Zirconia-based dental ceramics. Dent. Mater. 20 (5), 449–456, http://dx.doi.org/10.1016/j.dental.2003.05.002.

Guess, P.C., Zhang, Y., Kim, J.W., Rekow, E.D., Thompson, V.P., 2010. Damage and reliability of Y-TZP after cementation surface treatment. J. Dent. Res. 89 (6), 592–596, http://dx.doi.org/10.1177/0022034510363253.

Hjerppe, J., Fröberg, K., Lassila, L.V.J., Vallittu, P.K., 2010. The effect of heat treatment and feldspathic glazing on some mechanical properties of zirconia. Silicon 2, 171–178, http://dx.doi.org/10.1007/s12633-010-9042-y.

Kitayama, S., Nikaido, T., Maruoka, R., Zhu, L., Ikeda, M., Watanabe, A., Foxton, R.M., Miura, H., Tagami, J., 2009. Effect of an internal coating technique on tensile bond strengths of resin cements to zirconia ceramics. Dent. Mater. J. 28 (4), 446–453, http://dx.doi.org/10.4012/dmj.28.446.

Kosmac, T., Wagner, R., Claussen, N., 1981. X-ray determination of transformation depths in ceramics containing tetragonal $ZrO_2$. J. Am. Ceram. Soc. 64 (4), C72–C73, http://dx.doi.org/10.1111/j.1151-2916.1981.tb10285.x.

Kosmac, T., Oblak, C., Marion, L., 2008. The effects of dental grinding and sandblasting on ageing and fatigue behavior of dental zirconia (Y-TZP) ceramics. J. Eur. Ceram. Soc. 28 (5), 1085–1090, http://dx.doi.org/10.1016/j.jeurceramsoc.2007.09.013.

Luthardt, R.G., Holzhüter, M., Sandkuhl, O., Herold, V., Schnapp, J. D., Kuhlisch, E., Walter, M., 2002. Reliability and properties of ground Y-TZP-zirconia ceramics. J. Dent. Res. 81 (7), 487–491, http://dx.doi.org/10.1177/154405910208100711.

Luthardt, R.G., Holzhuter, M.S., Rudolph, H., Herold, V., Walter, M. H., 2004. CAD/CAM-machining effects on Y-TZP zirconia. Dent. Mater. 20 (7), 655–662, http://dx.doi.org/10.1016/j.dental.2003.08.007.

Mitov, G., Gessner, J., Lohbauer, U., Woll, K., Muecklich, F., Pospiech, P., 2011. Subcritical crack growth behavior and life data analysis of two types of dental Y-TZP ceramics. Dent. Mater. 27 (7), 684–691, http://dx.doi.org/10.1016/j.dental.2011.03.010.

Morena, R., Beaudreau, G.M., Lockwood, P.E., Evans, A.L., Fairhurst, C.W., 1986. Fatigue of dental ceramics in a simulated oral environment. J. Dent. Res. 65 (7), 993–997, http://dx.doi.org/10.1177/00220345860650071901.

Näpänkangas, R., Pihlaja, J., Raustia, A., 2015. Outcome of zirconia single crowns made by predoctoral dental students: a clinical retrospective study after 2 to 6 years of clinical service. J. Prosthet. Dent. 113 (4), 289–294, http://dx.doi.org/10.1016/j.prosdent.2014.09.025.

Ntala, P., Chen, X., Niggli, J., Cattell, M., 2010. Development and testing of multi-phase glazes for adhesive bonding to zirconia substrates. J. Dent. 38, 773–781, http://dx.doi.org/10.1016/j.jdent.2010.06.008.

Quinn, G.D., 2007. NIST Recommended Practice Guide: Fractography of Ceramics and Glasses. National Institute of Standards and Technology, United States.

Ritter, J.E., Humenik, J.N., 1979. Static and dynamic fatigue of polycrystalline alumina. J. Membr. Sci. 14, 1573–4803, http://dx.doi.org/10.1007/BF00772723.

Scherrer, S.S., Cattani-Lorente, M., Vittecoq, E., de Mestral, F., Griggs, J.A., Wiskott, H.W., 2011. Fatigue behavior in water of Y TZP zirconia ceramics after abrasion with 30 μm silica-coated alumina particles. Dent. Mater. 27 (2), e28–e42, http://dx.doi.org/10.1016/j.dental.2010.10.003.

Souza, R.A.O., Valandro, L.F., Melo, R.M., Machado, J.P.B., Bottino, M.A., Özcan, M., 2013. Air-particle abrasion on zirconia ceramic using different protocols: effects on biaxial flexural strength after cyclic loading, phase transformation and surface topography. J. Mech. Behav. Biomed. Mater. 26, 155–163, http://dx.doi.org/10.1016/j.jmbbm.2013.04.018.

Stober, T., Bermejo, J.L., Rammelsberg, P., Schmitter, M., 2014. Enamel wear caused by monolithic zirconia crowns after 6 months of clinical use. J. Oral. Rehabil. 41 (4), 314–322, http://dx.doi.org/10.1111/joor.12139.

Taskonak, B., Griggs, J.A., Mecholsky, J.J., Yan, J.H., 2008. Analysis of subcritical crack growth in dental ceramics using fracture mechanics and fractography. Dent. Mater. 24 (5), 700–707, http://dx.doi.org/10.1016/j.dental.2007.08.001.

Teixeira, E.C., Piascik, J.R., Stoner, B.R., Thompson, J.Y., 2007. Dynamic fatigue and strength characterization of three ceramic materials. J. Mater. Sci. Mater. Med. 18 (6), 1219–1224, http://dx.doi.org/10.1007/s10856-007-0131-4.

Toraya, H., Yoshimura, M., Somiya, S., 1984. Calibration curve for quantitative analysis of the monoclinic-tetragonal $ZrO_2$ system by x-ray diffraction. J. Am. Ceram. Soc. 67 (6), C119–C121, http://dx.doi.org/10.1111/j.1151-2916.1984.tb19715.x.

Vanderlei, A., Bottino, M., Valandro, L.F., 2014. Evaluation of resin bond strength to yttria-stabilized tetragonal zirconia and framework marginal fit: comparison of different surface conditionings. Oper. Dent. 39 (1), 50–63, http://dx.doi.org/10.2341/12-269-L.

Wang, H., Aboushelib, M.N., Feilzer, A.J., 2008. Strength influencing variables on CAD/CAM zirconia frameworks. Dent. Mater. 24 (5), 633–638, http://dx.doi.org/10.1016/j.dental.2007.06.030.

Wiskott, H.W., Nicholls, Jl, Belser, U.C., 1995. Stress fatigue: basic principles and prosthodontic implications. Int. J. Prosthodont. 8 (2), 105–116.

Zhang, Y., Pajares, A., Lawn, B.R., 2004. Fatigue and damage tolerance of Y-TZP ceramics in layered biomechanical systems. J. Biomed. Mater. Res. B Appl. Biomater. 71 (1), 166–171, http://dx.doi.org/10.1002/jbm.b.30083.

Zhang, Y., Lawn, B.R., Malament, K.A., Van Thompson, P., Rekow, E.D., 2006. Damage accumulation and fatigue life of particle-abraded ceramics. Int. J. Prosthodont. 19 (5), 442–448.